Lab on a Chip

COMMUNICATION

View Article Online
View Journal | View Issue

Cite this: *Lab Chip*, 2024, **24**, 4232

Received 10th May 2024,
Accepted 20th August 2024

DOI: 10.1039/d4lc00413b

rsc.li/loc

Single cell glucose-stimulated insulin secretion assay using nanowell-in-microwell plates†

Deasung Jang,[ab] Kerryn Matthews,[ab] Pan Deng,[ab] Samuel G. Berryman,[ab] Cuilan Nian,[cd] Simon P. Duffy,[e] Francis C. Lynn[cdf] and Hongshen Ma *[abfg]

Pancreatic β cells secrete insulin in response to elevated levels of glucose. Stem cell derived β (SCβ) cells aim to replicate this glucose-stimulated insulin secretion (GSIS) function, but current preparations cannot provide the same level of insulin as natural β cells. Here, we develop an assay to measure GSIS at the single cell level to investigate the functional heterogeneity of SCβ cells and donor-derived islet cells. Our assay involves randomly depositing single cells and insulin capture microbeads in open-top nanowells (40 × 40 × 55 μm^3) fabricated on glass-bottom imaging microwell plates. Insulin secreted from single cells is captured on microbeads and then stained using a detection antibody. The nanowell microstructure limits diffusion of secreted insulin. The glass substrate provides an optically flat surface for quantitative microscopy to measure the concentration of secreted insulin. We used this approach to measure GSIS from SCβ cells and donor-derived islet cells after 15 minutes exposure to 3.3 mM and 16.7 mM glucose. Both cell types exhibited significant GSIS heterogeneity, where elite cells (<20%) produced the majority of the secreted insulin (55–78%). This assay provides an immediate readout of single cell glucose-stimulated insulin secretion in a flexible well plate-based format.

Introduction

Pancreatic beta (β) cells, residing in the islets of Langerhans, manage blood glucose levels through their glucose-stimulated insulin secretion (GSIS) function. Type 1 diabetes (T1D) is caused by autoimmune destruction of β cells resulting in insulin deficiency. T1D can be treated with lifelong insulin injections, but this treatment must be carefully matched to blood glucose levels to maintain glycemic balance.[1–3] Using the Edmonton protocol to transplant islets from deceased donors to the liver portal vein can provide robust glycemic control without insulin injection.[4] However, the limited availability of cadaveric donor islets cannot meet the demand for all T1D patients.[5] Additionally, the life span of transplanted islets is limited, with fewer than 50% of recipients maintaining insulin independence after five years, and therefore requiring additional transplantations.[5–8] Consequently, there is a critical need for new sources of β cells. Significant progress has been made in the differentiation and genetic engineering of pluripotent stem cells into stem cell derived β (SCβ) cells to provide a limitless supply of insulin-producing cells. However, current protocols produce SCβ cells with varying degrees of functional maturity that collectively provide GSIS at ~30% of the level of donor islets.[9,10]

One approach to investigate the discrepancy in GSIS between SCβ and primary β cells is to analyze the molecular and functional heterogeneity of these cells. Some approaches aim to define the molecular biomarkers of mature β cells through transcriptome[11–13] and antigen profiling.[14] Transcriptomics describes that the β cell population can be subdivided into distinct clusters that vary in insulin expression[15] as well as genes associated with metabolism and cell maturation.[11] Antigen profiling has similarly identified distinct β cell subsets, including ST8SIA1+ β cell subpopulations that are less responsive to glucose.[14]

Functional heterogeneity of β cells has been investigated using GFP reporter systems to measure differences in protein expression,[16–20] as well as insulin exocytosis from single β-cells

[a] *Department of Mechanical Engineering, University of British Columbia, Vancouver, BC, Canada. E-mail: hongma@mech.ubc.ca*
[b] *Centre for Blood Research, University of British Columbia, Vancouver, BC, Canada*
[c] *BC Children's Hospital Research Institute CFKF Diabetes Research Program, Vancouver, BC, Canada*
[d] *Department of Surgery, Faculty of Medicine, University of British Columbia, Vancouver, BC, Canada*
[e] *British Columbia Institute of Technology, Canada*
[f] *School of Biomedical Engineering, University of British Columbia, Vancouver, BC, Canada*
[g] *Vancouver Prostate Centre, Vancouver General Hospital, Vancouver, BC, Canada*
† Electronic supplementary information (ESI) available. See DOI: https://doi.org/10.1039/d4lc00413b

measured using amperometric monitoring,[21] fluorogenic tracers,[22] and calcium flux.[23] However, none of these strategies can measure the functional heterogeneity of GSIS in single β cells. To investigate GSIS on small numbers of cells, previous studies have developed perfusion microfluidic devices to measure insulin secretion from individual islets.[24,25] These devices provided precise measurements of the dynamic insulin response to glucose stimulation, but are impractical for functional single cell measurements.

A key limitation of current β cell heterogeneity profiling is that the abundance of secreted insulin depends on post-translational processing of the protein and its accumulation within secretory granules, which cannot be assessed by quantifying gene expression.[26] Consequently, none of these current methods can directly quantify GSIS at the single-cell level in order to understand how each cell contributes to the overall secretory profile. When considering how single cell GSIS may be distributed for both SCβ cells and primary β cells, it is possible to imagine three scenarios: (1) homogeneous – where all cells contribute around a mean level of GSIS, perhaps distributed as a Gaussian; (2) discretely heterogeneous – where only a sub-population of β cells exhibit GSIS function, while the remaining β cells are inactive; (3) Continuously heterogeneous – where the amount of GSIS is distributed over a wide range of values across the individual β cells. Understanding the character of this heterogeneity, as well as the differences between SCβ cell and primary β cells, will provide important clues on how SCβ cell design and engineering could be improved to elicit greater GSIS.

Here, we developed a nanowell-based single cell assay to directly quantify insulin secretion in β cells. This assay builds on our previous nanowell technology that uses laser-induced polymerization to generate high-aspect ratio nanowells on glass surfaces to limit the diffusion of secreted factors between nanowells.[27] Our assay involves co-depositing β cells with insulin-capture magnetic microparticles, stimulating the β cells with glucose, and then measuring the secreted insulin by immunofluorescence. We observed that both SCβ cells and islet-derived β cells exhibit a remarkable degree of secretion heterogeneity, with a small fraction of elite cells responsible for the majority of the GSIS response, consistent with the continuously heterogeneous model for β cell functional heterogeneity. Our findings further suggest that the differences in GSIS between SCβ and primary β cells may be the fidelity of the elite GSIS cells, and that further genetic engineering efforts should aim to favor the development of these cells.

Results

Approach

Our approach for measuring the GSIS function of β cells at the single cell level is to deposit single cells in open-top nanowells fabricated inside the microwells of a standard 384-well glass-bottom imaging plate (Fig. 1A). These nanowell-in-

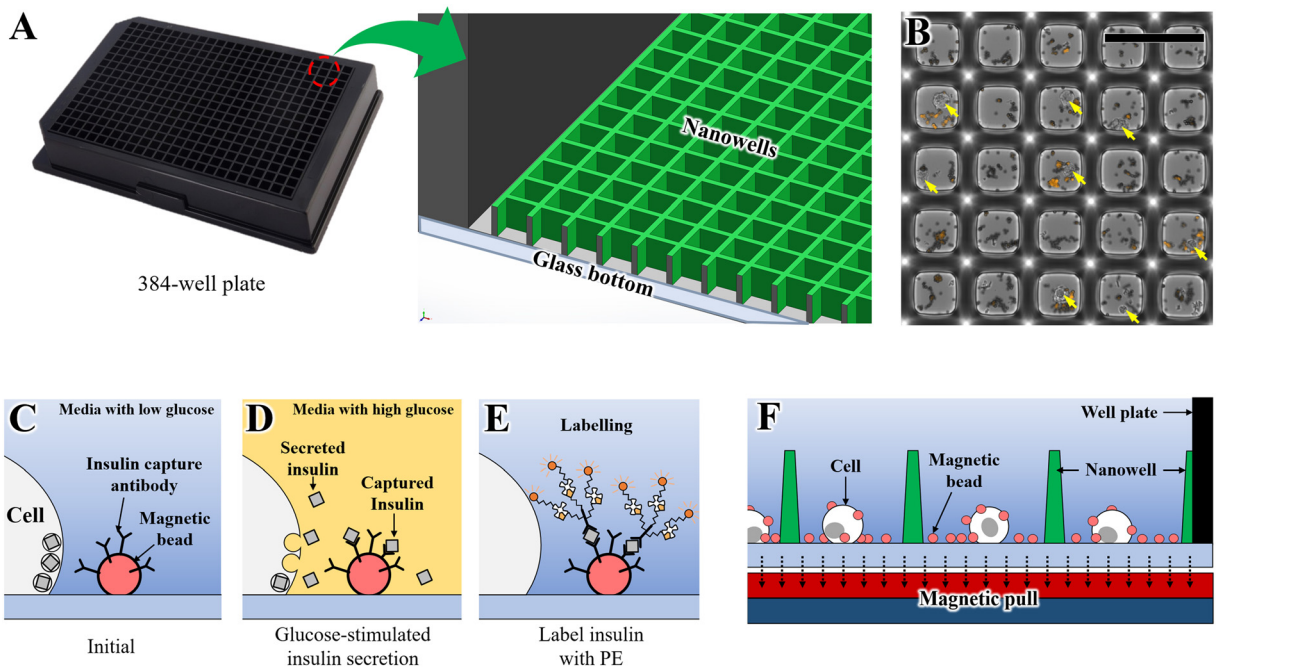

Fig. 1 Overall schematic of single β-cell glucose-stimulated insulin secretion (GSIS) assay using nanowells in a microwell. (A) Nanowell array is fabricated in a standard 384-well plate. (B) A representative image of single cells and beads in the nanowell array. Scale bar = 100 μm. The positions of cells are indicated as yellow arrows. (C) Single cells are co-deposited with magnetic beds that are functionalized with antibodies specific to insulin. Under low glucose conditions, little insulin adsorbs to the beads. (D) Under high glucose conditions, a greater amount of secreted insulin is adsorbed to the functionalized beads. (E) Detection of captured insulin is achieved by sandwich immunoassay, where insulin is bound by biotinylated anti-insulin and fluorescence signal is generated by streptavidin–phycoerythrin. (F) During all steps of the assay, a magnetized surface and high aspect nanowell walls ensure that beads are retained within the nanowell.

microwells have a pitch of 60 μm with internal dimensions of 40 × 40 × 55 μm ($l \times w \times h$). Each 3.2 × 3.2 mm microwell (from a 384-well plate) contains ~2500 nanowells.

The process for measuring glucose-stimulated insulin secretion from single β cells involves depositing these cells at 25–30% of the number of nanowells in order to maximize the number of nanowells occupied by a single cell based on Poisson distribution (Fig. 1B). These cells are co-deposited with 2.8 μm tosyl-activated magnetic beads that are covalently conjugated with insulin capture antibodies (Fig. 1C). The number of deposited insulin-capture beads is tuned so that at least 5 beads are found in each nanowell, in order to provide redundancy in the insulin secretion measurement. An important feature of our nanowell design is the high aspect ratio nanowells that allow cells and beads to be retained during reagent exchange, and localizes secreted molecules within the timeframe of the secretion assay.

After depositing the cells and beads in nanowells, glucose is added to stimulate the β cells. During a 15-minute incubation, secreted insulin molecules are captured on beads (Fig. 1D), and then subsequently immunostained for quantification by a sandwich assay, similar to an ELISA (Fig. 1E). Specifically, the captured insulin molecules are then labeled using a biotinylated detection antibody, which is subsequently tagged using streptavidin conjugated with phycoerythrin (PE). A magnet is used to help retain beads during the washing steps required for immunostaining (Fig. 1F). Finally, images of cells and beads are analyzed to identify nanowells that contain single cells, and to assess the fluorescence intensity of the beads in these nanowells.

Nanowell microfabrication

In order to enable high quality imaging and quantification insulin adsorption to capture beads, we fabricated the nanowell microstructure on a glass slide substrate using photolithography of a polyurethane-based polymer. The polymer is spin-coated on a silanized glass slide substrate, which deposits a ~500 μm thick layer. Photolithography is performed using a photomask from the bottom side of the glass slide because, unlike traditional photoresist, this polymer remains in liquid form after deposition. The height of the nanowell walls is determined by the UV exposure dosage, which we determined experimentally to obtain a thickness of ~55 μm. The bottom side exposure approach also provided a favorable tapered shape of the nanowell walls to facilitate efficient reagent exchange.

Cell and bead retention during reagent exchange

We performed experiments to confirm the retention of single cells and beads in nanowells during reagent exchange. We deposited SCβ and 2.8 μm diameter insulin capture beads into nanowells, and then quantified their numbers using automated image analysis (Fig. 2A). To track their initial positions, SCβ cells were labelled with GFP and Hoechst stain and we observed autofluorescence of the beads in the cyanine-5 channel. Insulin was added to the microwell and adsorbed to the capture beads, followed by immunofluorescence staining with biotinylated anti-insulin and PE–streptavidin. This procedure involved staining the beads with biotinylated anti-insulin and streptavidin–PE,

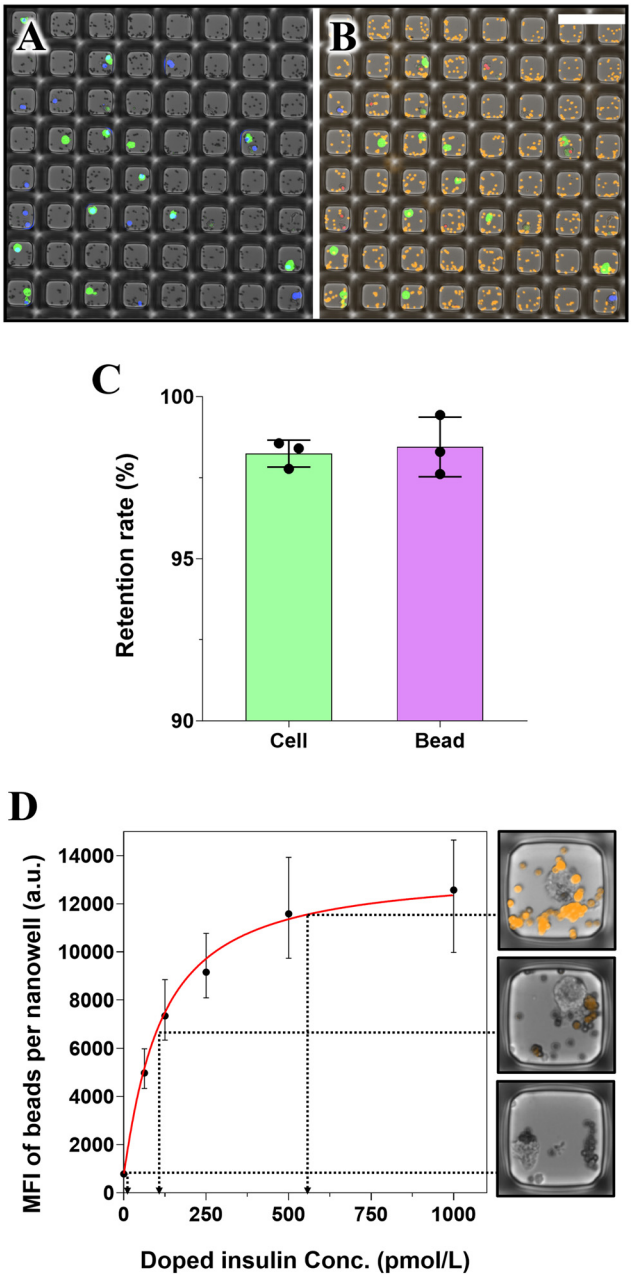

Fig. 2 Validation of a nanowell array and insulin capture beads for single β-cell GSIS assays. (A) Cells (green) and beads (red) can be visualized before immunostaining. (B) The positions of cells and beads are unchanged following immunostaining. Scale bar = 100 μm. (C) Cells and beads are retained within the nanowell at rates of 98.3% and 98.5% respectively (n = 3). The dots and error bars here indicate the result of each retention test and the range of data, respectively. (D) The standard curve for insulin capture beads shows a good correlation between the concentration of insulin and fluorescence intensity of beads. The dots and error bars indicate the median and interquartile range, respectively.

which included four washes with an electronic pipette. All steps of this procedure were performed on a magnetic surface to retain the magnetic beads inside the nanowell. We then re-imaged the nanowells to quantify the numbers of cells and beads in each nanowell. Through this process, we show that SCβ cells and beads were retained at a rate of 98.3% and 98.5% respectively, across three replicates (Fig. 2C). These results confirm that the nanowells can effectively retain single cells and beads throughout the assay.

Insulin capture bead testing

To convert the fluorescent intensity measured from images of immunostained insulin-capture beads into corresponding insulin concentrations, we constructed a standard curve using doped insulin. Specifically, we exposed beads to insulin dilutions ranging from 0 to 1000 pM (Fig. 2D). These beads were then deposited into the nanowell array, immunostained, and assessed using microscopy. To account for variability between beads, the mean fluorescence intensity (MFI) of the capture beads in each nanowell was averaged to obtain an overall intensity value for each nanowell. Measurements for each standard curve were obtained from 500 nanowells, which were selected from the center and each of the four corners of the same nanowell. The resulting standard curve showed an expected increase in fluorescence intensity with insulin concentration from 0 pM up to 1000 pM, corresponding to an escalating fluorescent intensity of the

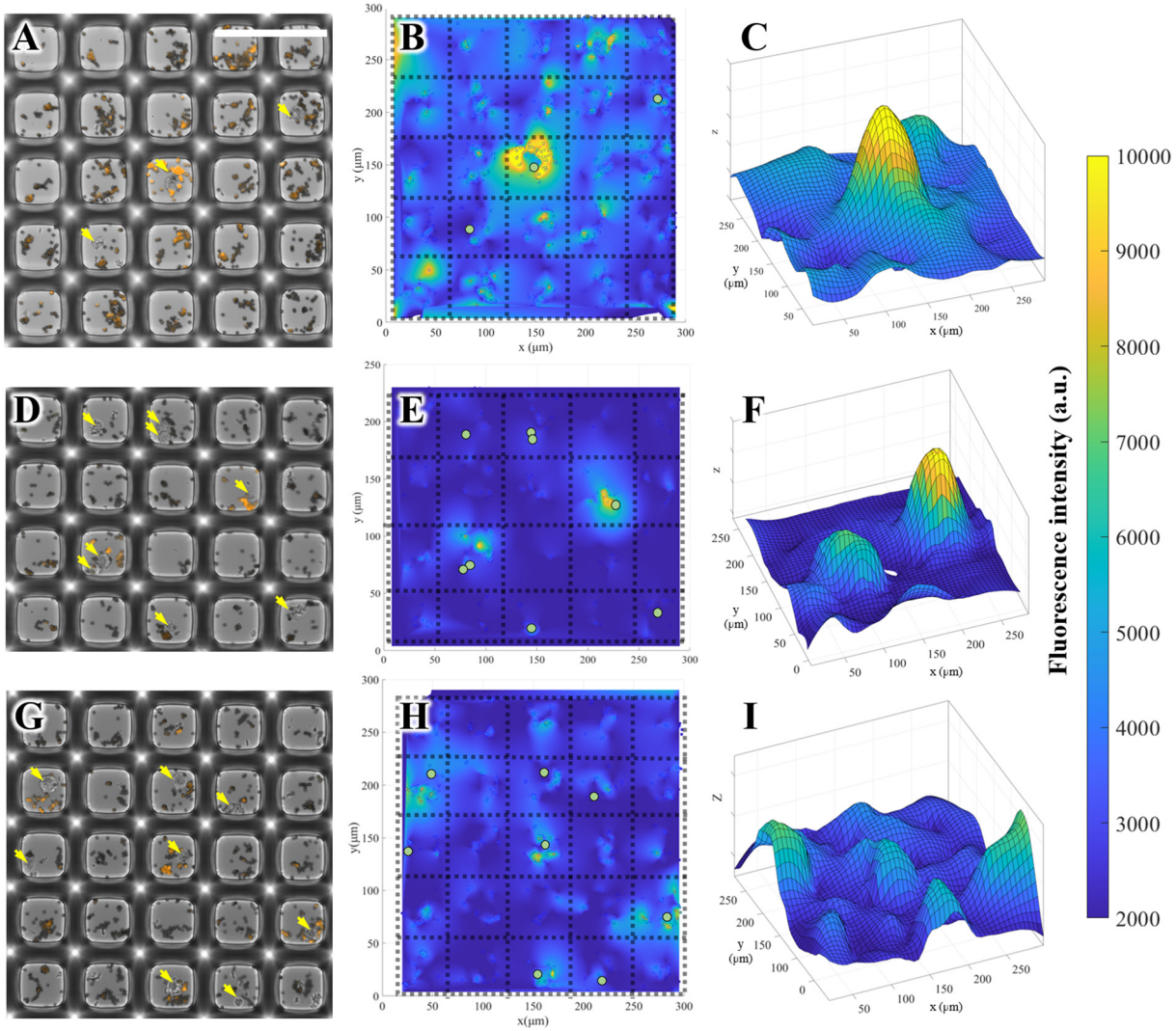

Fig. 3 Confinement of secreted insulin within nanowells. Single SCβ cell insulin secretion after 15 min glucose (16.7 mM) stimulation is measured *via* bead fluorescence intensity in the microscopic images. Representative microscopic images show (A) a high secreting cell near non-secreting cells, (D) moderate secreting cells near non-secreting cells, and (G) low and non-secreting cells. (A, D and G) The left images are brightfield images overlaid with fluorescence of the insulin detection antibody. Cells are indicated as yellow arrows. (B, E and H) The middle images are 2D heatmaps generated from fluorescence intensity of the insulin capture beads. The green dots and dotted lines indicate the position of cells and wall of the nanowell, respectively. (C, F and I) The right images show the heat map data fitted to Gaussian distributions around each cell. *X* and *Y* axis units are μm and *Z* axis is the fluorescence intensity. Scale bar = 100 μm. Fluorescence images were captured with 1× gain and 500 ms exposure.

beads from 782 ± 35.39 to 12 216 ± 2768 a.u (mean ± SD). The limit of detection for the assay was obtained as 0.04 pM, as determined from the standard deviation from the mean at the 0 pM data point. These results confirm the ability to use insulin capture beads to measure insulin concentration.

Confinement of single cell secretion to individual nanowells

We performed an experiment to determine whether secreted insulin molecules are confined to individual nanowells within the 15-minute time frame of the assay. This experiment involved depositing SCβ cells at low density while depositing insulin-capture beads at normal density. This arrangement allowed us to identify instances of single cells isolated from other cells by several rows and columns of nanowells. We can then use the insulin-capture bead fluorescence to map the spread of secreted insulin from these isolated single cells to determine the spread distance. Fig. 3 shows representative results from several situations including a single high-secreting cell (Fig. 3A), two nearby high-secreting cells (Fig. 3D), and multiple secreting cells (Fig. 3G). Visualizing these cases as a 2D heatmap (Fig. 3B, E and H) as well as a 3D Gaussian plot (Fig. 3C, F and I) based on the fluorescence intensity data from beads in the nanowells, we can see that the secreted molecules were largely confined to individual nanowells, and the amount of secretion can be measured from the mean fluorescence intensity of the beads located in the same nanowell as the cell.

Single cell GSIS for SCβ and primary islet cells

We performed single cell GSIS assays on both SCβ cells and primary islet cells. In each assay, disaggregated cells and insulin capture beads were randomly deposited in a nanowell array and exposed to various glucose stimulation conditions within each microwell. To investigate the effect of disaggregation, which can induce cellular stress, we assayed both sets of cells in two ways: immediately after cell

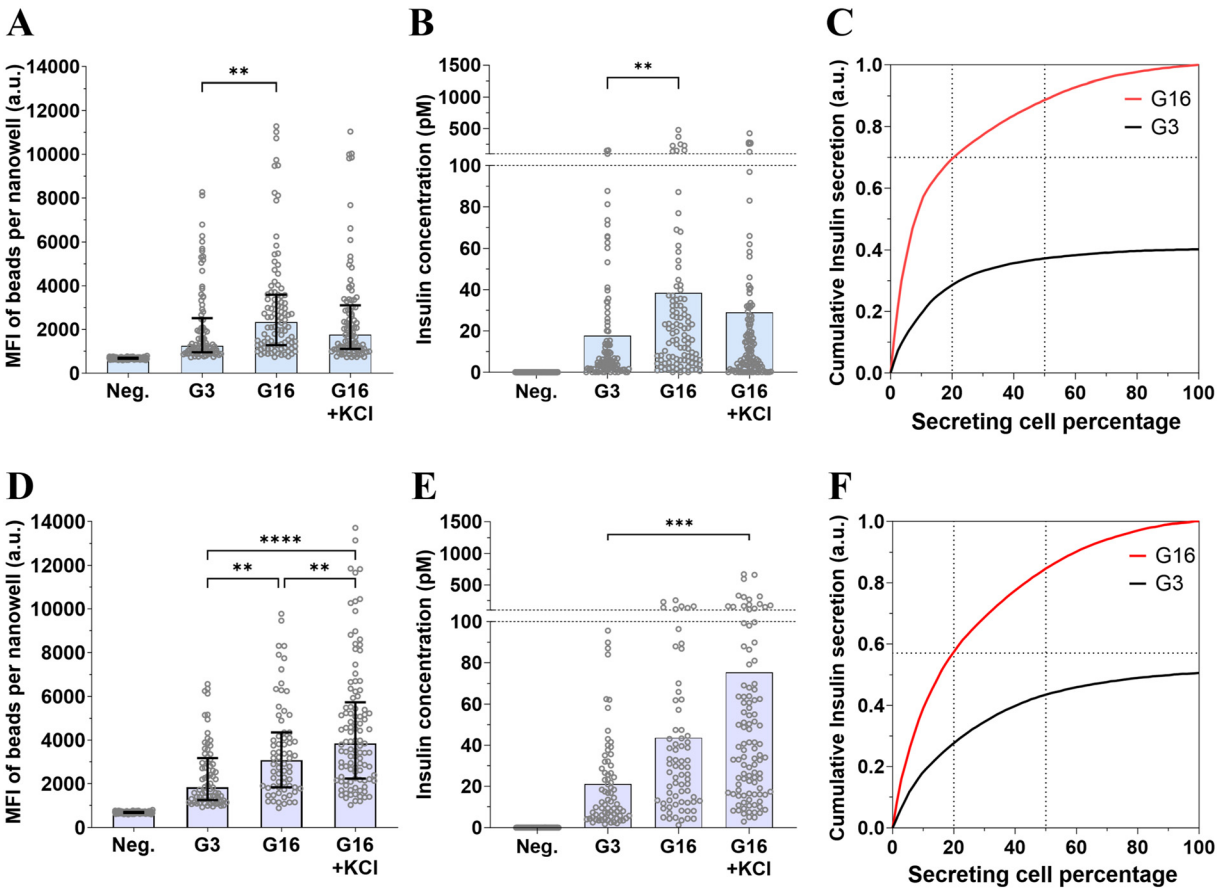

Fig. 4 Single SCβ cell GSIS assay. GSIS assay was performed (A–C) immediately after the cell dissociation or (D–F) 2 hours after cell dissociation. SCβ cells were stimulated with 3 mM glucose (G3) or 16.7 mM glucose (G16). Jurkat cells in 16.7 mM glucose served as negative controls (Neg.) and SCβ cells in 16.7 mM glucose and 40 mM KCl served as positive controls (G16 + KCl). (A and D) Mean fluorescence intensity (MFI) of beads averaged per nanowell measured in different glucose stimulations. The bar and error bar indicate median and interquartile range. (B and E) The bead MFI values are converted to insulin concentration using the standard curve of insulin capture bead. The results show high heterogeneity in β-cell function. The bar indicates the mean value. Positive controls with 2-hour cell resting exhibit higher insulin secretion than those assayed immediately after disaggregation. (C and F) Cumulative insulin secretion amount with respect to the secreting cell percentage arranged in the descending order of insulin secretion amount. It shows that the top 20% of secreting cells are responsible for 55–70% of total secretion amount. The significance levels for p-values are denoted as follows: $p < 0.05$ (*), 0.01 (**), 0.001 (***), 0.0001 (****).

dissociation (without resting) and after a 2-hour resting period following cell dissociation, using the same batch of cells.

For our single cell GSIS assays on SCβ cells, these cells were seeded into nanowells and either immediately stimulated with glucose (Fig. 4A–C) or glucose-stimulated after 2 hours of acclimatization to culture (Fig. 4D–F). Stimulation conditions for SCβ cells included low glucose (3 mM) for the basal secretion level, high glucose (16.7 mM), high glucose with 40 mM potassium chloride (KCl) for a positive control, and high glucose with non-insulin-secreting cells (Jurkat cells) for a negative control. Following a 15 min incubation in each condition, we immunostained the insulin capture beads and obtained images of the stained beads using automated microscopy.

We analyzed images of nanowells containing a single cell and multiple beads and measured the average mean fluorescence intensity (MFI) from beads per nanowell. This approach is based on the reasoning that some degree of mixing occurs within the nanowell. By averaging the MFI values across these beads, we achieved a representative value of the amount of secreted insulin, helping to account for any potential variability among individual beads. (Fig. 4A and D). These MFI values were then converted into insulin concentrations using a standard curve for the insulin capture beads (Fig. 4B and E).

Our results revealed that GSIS in SCβ cells exhibits considerable heterogeneity across all conditions, except for the negative control. The stimulation indexes, representing the fold change in insulin secretion under high glucose relative to low glucose, were 2.38 ± 0.26 for the assay without cell resting and 2.06 ± 0.19 for the assay with 2-hour cell resting, indicating no significant difference between the two assay methods. However, it's worth noting that the positive control exhibited 2.6 fold higher insulin secretion level with 2-hour resting compared to the assay without cell resting. We generated a cumulative insulin amount curve based on the percentage of secreting cells arranged in descending order of insulin secretion amount

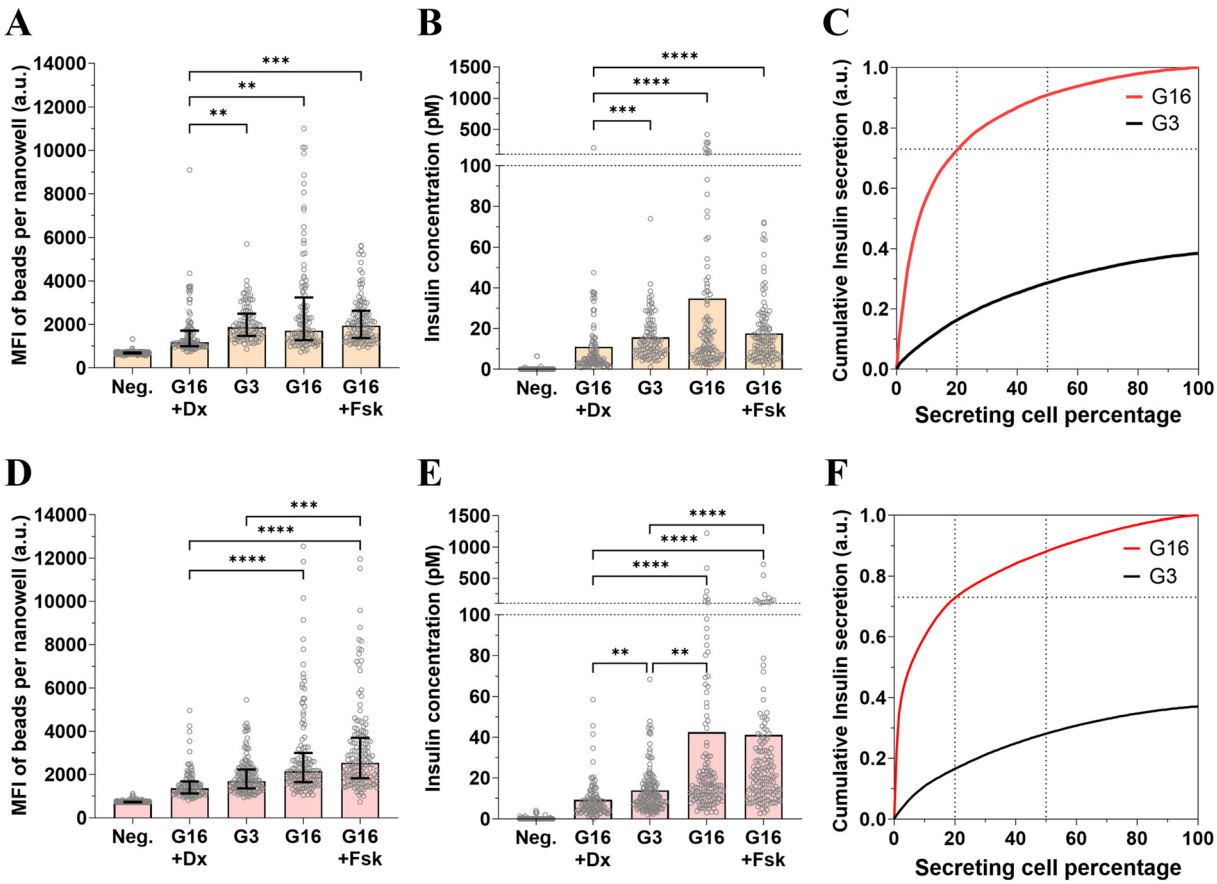

Fig. 5 Donor islet single cell GSIS assay. GSIS assay was performed (A–C) immediately after the cell dissociation or (D–F) 2 hours after cell dissociation. SCβ cells were stimulated with 3 mM glucose (G3) or 16.7 mM glucose (G16). Jurkat cells in 16.7 mM glucose and 100 μM diazoxide served as negative controls (Neg.) and SCβ cells in 16.7 mM glucose and 1 μM forskolin served as positive controls (G16 + Fsk). (A and D) Mean fluorescence intensity (MFI) of beads averaged per nanowell measured in different glucose stimulations. The bar and error bar indicate median and interquartile range. (B and E) The bead MFI values are converted to insulin concentration using the standard curve of insulin capture bead. The results show high heterogeneity in β-cell function. The bar indicates the mean value. Positive controls with 2-hour cell resting exhibit higher insulin secretion than those assayed immediately after disaggregation. (C and F) Cumulative insulin secretion amount with respect to the secreting cell percentage arranged in the descending order of insulin secretion amount. It shows that the top 20% of secreting cells are responsible for ~75% of total secretion amount. The significance levels for p-values are denoted as follows: $p < 0.05$ (*), 0.01 (**), 0.001 (***), 0.0001 (****).

(Fig. 4C and F). The curve highlighted that the top 20% of secreting cells account for approximately 55 to 68% of the total secretion, confirming the significant heterogeneity in the GSIS function across SCβ cells.

For primary donor islet cells, we seeded disaggregated cells into nanowells and either immediately stimulated with glucose (Fig. 5A–C) or glucose-stimulated after 2 hours of acclimatization to culture (Fig. 5D–F). The stimulation conditions of these cells included low glucose (3 mM) for basal secretion level, high glucose (16.7 mM), high glucose with 1 μM forskolin for the positive control, high glucose with non-insulin-secreting cells (Jurkat cells) for negative control, and high glucose with 100 μM diazoxide to reduces the insulin secretion by maintaining the cell in a hyperpolarized state inhibiting the calcium influx necessary for the exocytosis of insulin (Fig. 5). We followed the same procedure as with SCβ cells, measuring MFI values of beads per nanowell (Fig. 5A and D) and converting them to insulin concentrations (Fig. 5B and E). The stimulation indexes for the assays with and without cell resting were 3.05 ± 0.81 and 2.23 ± 0.19, respectively, indicating higher values with the 2-hour cell resting period. Interestingly, similar to the SCβ cells, the positive control exhibited a 2.3 fold higher insulin secretion level in the assay with 2-hour cell resting. The cumulative insulin amount curve for the donor islet cells showed that the top 20% of secreting cells contributed to approximately 75 to 78% of the total secretion (Fig. 5C and F), suggesting even greater heterogeneity compared to SCβ cells.

Discussion

Sealed nanoliter chambers have been previously developed to measure cytokine secretion from immune cells. However, infusing single cells into these chambers and exchanging media require a significant time delay,[28–30] which is more than the incubation time for GSIS experiments (typically <2 hours). Open-top nanowells can dramatically simplify and expedite the process for cell deposition, as well as subsequent reagent exchange, but previous fabrication methods relied on replica molding of PDMS, which introduced several inherent limitations. First, replica molding is limited in its ability to form thin-walled nanowells, which limit the density of the nanowell array. Importantly, thick nanowell walls create significant potential for cells to be deposited perched on top of the nanowell walls instead of inside nanowells. Second, replica molding imprints nanowell features into a PDMS membrane substrate. The thickness of this membrane cannot be precisely controlled and is usually non-uniform. As a result, it is often difficult to maintain a consistent focal plane to perform quantitative fluorescence imaging of cells and beads. Finally, many secreted proteins will non-specifically adsorb on the surface of PDMS, or absorb inside PDMS, which creates a fluorescence background signal that limits the sensitivity of quantitative imaging.

To overcome the challenges of open-top PDMS nanowell systems, as well as to develop an assay specifically for measuring single cell GSIS, we developed a process for photolithographic fabrication of open-top nanowells directly on glass substrates in standard format microwell plates. Our photolithographic process produces high aspect ratio nanowells that can retain cells and insulin capture beads during reagent exchange (required for stimulation, staining, and microscopy), as well as can confine secreted proteins within each nanowell. The photolithographic process also produces nanowells with thin walls to enable high density nanowell arrays in standard microwells. Specifically, ~2500 nanowells can be fabricated in each 3.2 × 3.2 mm microwell in a 384-well plate. Fabricating nanowells directly on a glass surface, allows cells and beads to be aligned to a consistent focal plane to enable quantitative fluorescence imaging. Finally, unlike PDMS, both the glass substrate and the nanowell polymers exhibit low protein adsorption.

Using our nanowell assay to profile SCβ cells and donor islet cells, we found that both cell types exhibited significant heterogeneity in their single cell GSIS. The character of this heterogeneity appears to be of the continuously heterogeneous case, where each sample contains cells with a wide range of GSIS levels. Notably, the total insulin secretion is dominated by a relatively small group of elite cells, whereby the top 20% insulin secreting cells produced 55–68% of total insulin from SCβ cell and 75–78% of the total insulin from donor islets cells. This finding suggests that the SCβ cells do not have a markedly different GSIS heterogeneity as donor islet cells, and that developing SCβ cells with greater GSIS likely involves increasing the number and potency of the elite insulin secreting cells.

Our finding inspires many follow up questions for subsequent research. First, is the single cell GSIS function for both elite and non-elite secretors persistent, or could this characteristic be altered or dynamic over time? If single cell GSIS can be altered, what factors (*i.e.* secretagogues) might affect this property? Second, what are the effects of neighboring cells? Our study was performed by disaggregating SCβ cells and donor islet cells into single cell suspensions, which eliminates communications between neighboring cells that may coordinate the GSIS response.[31,32] The effect of neighboring cells could perhaps be studied by assessing GSIS of cell clusters with different cell numbers and cell compositions. Finally, is GSIS measured at the single cell level correlated with GSIS of SCβ cells and donor islets? If so, this single cell assay could provide a rapid and standardizable means to assess SCβ cell quality during the biomanufacturing of these cells prior to transplantation into patients.

Materials and methods

Nanowell fabrication

A glass slide (Schott D263T eco 75 × 50 × 0.5 mm^3, Abrisa) was prepared by washing with acetone and isopropyl alcohol (IPA) for 20 min each, followed by plasma cleaning by

hydroxylation for 2 min. The glass slide was subsequently treated with 10% v/v TMSPMA (M6514, Sigma-Aldrich) in ethanol for 2 h at 70 °C and washed with ethanol, and then baked at 80 °C for 1 h. Nanowells were microfabricated on the surface of the TMSPMA-treated glass slide using a photolithographic process. First, a prepolymer (436909, Sigma-Aldrich) was spin-coated on the glass slide at 500 rpm for 5 s and subsequently at 1000 rpm for 5 s. A chrome photomask patterned with features of 40 × 40 μm^2 was placed in contact with the glass slide, and UV light (20 mW cm^{-2}) was irradiated for 1 s through the photomask. After UV irradiation, the nanowell-pattered glass was rinsed with 100% IPA to wash out the uncured prepolymer residue in nanowells for 15 min, followed by a post-curing process for 15 min under UV irradiation. Finally, the glass slide patterned with nanowells was assembled with a bottomless 384-well plate (206384, GraceBio).

Preparation of single β cells

Collection of and use of human donor islets and embryonic stem cells (ESC) was performed with informed consent and approved by the UBC Children's and Women's Research Ethics Board (H09-00676). Human donor islet cells were isolated from a male non-diabetic donor (age 33, BMI 22.2 kg m^{-2}, total IEQ 12 479) by the University of Alberta Clinical Cores as previously described.[33] SCβ cell spheroids were generated from an H1 cell line that was generously provided by WiCell (Madison, WI, USA) and used to generate a heterozygous INS-2A-GFP hESC clone and differentiated into SCβ cell spheroids, using protocols that have previously been described.[18,34,35] Donor islets and SCβ cell spheroids were collected in a 15 ml conical tube and incubated in disaggregation reagent (Accumax, StemCell Technologies) at 37 °C for 8 min with flicking the vial every 2 min. Disaggregation was terminated by washing the cells in 2.5 mL PBS, centrifugation at 200 g for 5 min and resuspension of the cells into media. The media used for disaggregated islet cells was CMRL 1066 (VWR, USA; CA45001-114) and the media used for SCβ cells was stage 7 media.[36] Single cells were obtained by filtering the cell suspension through 40 μm micropore sieve into fresh media. Cells were optionally incubated 2 h in media at 37 °C to allow cell recovery prior to GSIS assay. β cells were then incubated at 37 °C for 30 min in 3 mM glucose-supplemented media, allowing them to secret basal insulin level. Within that 30 min, cell nuclei were also stained with 5 μg mL^{-1} of Hoechst 33342 (Invitrogen).

Preparation of insulin capture beads

Insulin capture beads were prepared by covalent conjugation of anti-insulin (R&D systems) to tosyl-activated M-280 Dynabeads (ThermoFisher). The beads were washed twice with PBS and incubated in 36 μg ml^{-1} anti-insulin overnight at room temperature. After the overnight incubation, the beads were resuspended in 0.5% bovine serum albumin (BSA) in PBS and incubated for 1 h. The beads were washed twice and stored at 0.1% BSA in PBS until use.

Glucose stimulated insulin secretion

Disaggregated islet-derived β cells or SCβ cells suspended in 100 μl of 3 mM glucose solution were initially added in each microwell. Next, beads suspended in 2 μl of 0.1% BSA in PBS were deposited. After that, 98 μl of the solution was aspirated from the each microwell. Finally, 100 μl of stimulation reagent was added. The cells were suspended in Krebs-Ringer bicarbonate buffer (KRBH, Sigma-Aldrich), supplemented with either 3 mM or 16.7 mM glucose. As positive control, cells were supplemented with 16.7 mM glucose as well as 1 μM forskolin (islet-derived β cells) or 40 mM KCl (SCβ cells). Jurkat cells do not secrete insulin and were suspended in 16.7 mM glucose in KRBH as negative control. Glucose-stimulated cells were mixed with insulin capture beads seeded into the nanowell array and incubated for 15 min to permit insulin adsorption onto capture beads. Glucose stimulation was halted by removal of glucose through PBS wash at the end of the incubation period.

Immunostaining for insulin quantification

Following GSIS and adsorption of insulin onto tosyl-activated M-280 Dynabeads (ThermoFisher), insulin was quantified using the Human Insulin DuoSet ELISA kit (DY8056-05, R&D Systems). The nanowells were placed on a magnetized surface to retain beads during all steps of this procedure. The beads were washed with PBS and incubated with insulin-specific detection antibody (15 ng mL^{-1}) in PBS for 30 min at room temperature. Subsequently, the beads were again washed with PBS and incubated with streptavidin–PE (0.5 μg mL^{-1}) in PBS for 20 min at room temperature. Finally, the nanowells were washed twice with PBS to minimize the fluorescence background.

Image acquisition and analysis

Microscopy of cell and bead samples in nanowell-in-microwells was performed using a 20× objective (CFI S Plan Fluor ELWD 20XC, NA = 0.45, Nikon) on an inverted fluorescence microscope (Ti2-E, Nikon). All images were captured using a monochrome CMOS camera (DS-Qi2, Nikon). Fluorescence images were acquired with 1× gain and 500 ms exposure. The microwell contains ~2500 nanowells that were identified using a custom Python script. Each nanowell was subsequently assessed for Hoechst 33342 nucleus stain and nanowells with single nuclei were segmented from the original image. The segmented images were re-imported into microscopy software (NIS-element, Nikon) for detection of beads and measurement of bead fluorescence intensity. Batch image analysis was performed on the image set to acquire the mean fluorescence intensity of insulin capture beads in each nanowell.

Statistical analysis

Statistical analysis was performed with one-way ANOVA with Kruskal–Wallis test using Graphpad Prism v10.0. Statistical significance was accepted at $p < 0.05$.

Ethics approval statement

This study was approved by the University of British Columbia's and BC Children's and Women's Hospital Research Ethics Board (H09-00676).

Significance of the work

This article provides the first report of direct quantitative measurement of glucose-stimulated insulin secretion from single cells. Our results reveal the heterogeneity of single cell function for both stem cell derived beta cells and human islet cells.

Data availability

The data supporting this article have been included as part of the ESI.†

Author contributions

H. M. and F. C. L. conceptualized the study. D. J., S. G. B., K. M., and C. N. developed the methodology. D. J. and K. M. performed the study. C. N. generated the stem cell derived beta cells. D. J., P. D., K. M., and S. P. D. analyzed the data. D. J., K. M., S. P. D., H. M. and F. C. L. wrote and edited the manuscript.

Conflicts of interest

S. G. B. and H. M. have financial interest in ImageCyte Technologies, which is commercializing the nanowell-in-microwell plates. Some of the authors are inventors on patent applications owned by the University of British Columbia.

Acknowledgements

H. M. was supported by grants from JDRF (1-INO-2023-1338-A-N), Diabetes Canada (OG-3-23-5725-HM), Canadian Institutes of Health Research (183872), and Natural Sciences and Engineering Research Council of Canada (2020-05412, 2020-00530). F. C. L. was supported by grants from JDRF (5-SRA-2020-1059-S-B, 3-COE-2022-1103-M-B) and Canadian Institutes of Health Research (ASD-173663). F. C. L. received salary support from Michael Smith Foundation for Health Research (5238 BIOM) and the BC Children's Hospital Research Institute (IGAP awards). P. D. was supported by awards from the China Scholarship Council and the Tai Hung Fai Charitable Foundation. S. G. B. was supported by awards from the Society for Laboratory Automation and Screening Graduate Education Fellowship and the UBC Four Year Doctoral Fellowship. The authors acknowledge that UBC and BC Children's Hospital are situated on the traditional, ancestral, and unceded territories of the Coast Salish peoples, the Sḵwx̱wú7mesh (Squamish), səl̓ilwətaʔɬ (Tsleil-Waututh), and xʷməθkʷəy̓əm (Musqueam) Nations.

References

1 K. M. Miller, N. C. Foster, R. W. Beck, R. M. Bergensta, S. N. DuBose and L. A. DiMeglio, *et al.*, Current state of type 1 diabetes treatment in the U.S.: Updated data from the t1d exchange clinic registry, *Diabetes Care*, 2015, **38**(6), 971–978.

2 R. W. Holl, P. G. F. Swift, H. B. Mortensen, H. Lynggaard, P. Hougaard and H. J. Aanstoot, *et al.*, Insulin injection regimens and metabolic control in an international survey of adolescents with type 1 diabetes over 3 years: Results from the Hvidore study group, *Eur. J. Pediatr.*, 2003, **162**(1), 22–29.

3 D. M. Nathan, Long-Term Complications of Diabetes Mellitus, *N. Engl. J. Med.*, 1993, **328**(23), 1676–1685.

4 A. M. J. Shapiro, State of the art of clinical islet transplantation and novel protocols of immunosuppression, *Curr. Diabetes Rep.*, 2011, **11**(5), 345–354.

5 A. M. J. Shapiro, M. Pokrywczynska and C. Ricordi, Clinical pancreatic islet transplantation, *Nat. Rev. Endocrinol.*, 2017, **13**(5), 268–277.

6 E. A. Ryan, B. W. Paty, P. A. Senior, D. Bigam, E. Alfadhli and N. M. Kneteman, *et al.*, Five-year follow-up after clinical islet transplantation, *Diabetes*, 2005, **54**(7), 2060–2069.

7 A. M. J. Shapiro, C. Ricordi, B. J. Hering, H. Auchincloss, R. Lindblad and R. P. Robertson, *et al.*, International Trial of the Edmonton Protocol for Islet Transplantation, *N. Engl. J. Med.*, 2006, **355**(13), 1318–1330.

8 B. A. Marfil-Garza, S. Imes, K. Verhoeff, J. Hefler, A. Lam and K. Dajani, *et al.*, Pancreatic islet transplantation in type 1 diabetes: 20-year experience from a single-centre cohort in Canada, *Lancet Diabetes Endocrinol.*, 2022, **10**(7), 519–532.

9 A. Rezania, J. E. Bruin, P. Arora, A. Rubin, I. Batushansky and A. Asadi, *et al.*, Reversal of diabetes with insulin-producing cells derived in vitro from human pluripotent stem cells, *Nat. Biotechnol.*, 2014, **32**(11), 1121–1133.

10 F. W. Pagliuca, J. R. Millman, M. Gürtler, M. Segel, A. Van Dervort and J. H. Ryu, *et al.*, Generation of functional human pancreatic β cells in vitro, *Cell*, 2014, **159**(2), 428–439.

11 D. Balboa, T. Barsby, V. Lithovius, J. Saarimäki-Vire, M. Omar-Hmeadi and O. Dyachok, *et al.*, Functional, metabolic and transcriptional maturation of human pancreatic islets derived from stem cells, *Nat. Biotechnol.*, 2022, **40**(7), 1042–1055.

12 Y. Xin, J. Kim, H. Okamoto, M. Ni, Y. Wei and C. Adler, *et al.*, RNA Sequencing of Single Human Islet Cells Reveals Type 2 Diabetes Genes, *Cell Metab.*, 2016, **24**(4), 608–615.

13 S. Tritschler, F. J. Theis, H. Lickert and A. Böttcher, Systematic single-cell analysis provides new insights into heterogeneity and plasticity of the pancreas, *Mol. Metab.*, 2017, **6**(9), 974–990.

14 C. Dorrell, J. Schug, P. S. Canaday, H. A. Russ, B. D. Tarlow and M. T. Grompe, *et al.*, Human islets contain four distinct subtypes of β cells, *Nat. Commun.*, 2016, **7**(1), 11756.
15 Å. Segerstolpe, A. Palasantza, P. Eliasson, E. M. Andersson, A. C. Andréasson and X. Sun, *et al.*, Single-Cell Transcriptome Profiling of Human Pancreatic Islets in Health and Type 2 Diabetes, *Cell Metab.*, 2016, **24**(4), 593–607.
16 A. K. Blöchinger, J. Siehler, K. Wißmiller, A. Shahryari, I. Burtscher and H. Lickert, Generation of an INSULIN-H2B-Cherry reporter human iPSC line, *Stem Cell Res.*, 2020, **45**, 101797.
17 S. J. Micallef, X. Li, J. V. Schiesser, C. E. Hirst, Q. C. Yu and S. M. Lim, *et al.*, INS(GFP/w) human embryonic stem cells facilitate isolation of in vitro derived insulin-producing cells, *Diabetologia*, 2012, **55**(3), 694–706.
18 G. G. Nair, J. S. Liu, H. A. Russ, S. Tran, M. S. Saxton and R. Chen, *et al.*, Recapitulating endocrine cell clustering in culture promotes maturation of human stem-cell-derived β cells, *Nat. Cell Biol.*, 2019, **21**(2), 263–274.
19 J. Siehler, A. K. Blöchinger, M. Akgün, X. Wang, A. Shahryari and A. Geerlof, *et al.*, Generation of a heterozygous C-peptide-mCherry reporter human iPSC line (HMGUi001-A-8), *Stem Cell Res.*, 2020, **50**, 102126.
20 C. M. J. Chu, H. Modi, C. Ellis, N. A. J. Krentz, S. Skovsø and Y. B. Zhao, *et al.*, Dynamic Ins2 Gene Activity Defines β-Cell Maturity States, *Diabetes*, 2022, **71**(12), 2612–2631.
21 R. T. Kennedy, L. Huang, M. A. Atkinson and P. Dush, Amperometric monitoring of chemical secretions from individual pancreatic beta-cells, *Anal. Chem.*, 1993, **65**(14), 1882–1887.
22 W. J. Qian, C. A. Aspinwall, M. A. Battiste and R. T. Kennedy, Detection of Secretion from Single Pancreatic β-Cells Using Extracellular Fluorogenic Reactions and Confocal Fluorescence Microscopy, *Anal. Chem.*, 2000, **72**(4), 711–717.
23 R. T. Scarl, K. L. Corbin, N. W. Vann, H. M. Smith, L. S. Satin and A. Sherman, *et al.*, Intact pancreatic islets and dispersed beta-cells both generate intracellular calcium oscillations but differ in their responsiveness to glucose, *Cell Calcium*, 2019, **83**, 102081.
24 P. M. Misun, B. Yesildag, F. Forschler, A. Neelakandhan, N. Rousset and A. Biernath, *et al.*, In Vitro Platform for Studying Human Insulin Release Dynamics of Single Pancreatic Islet Microtissues at High Resolution, *Adv. Biosyst.*, 2020, **4**(3), e1900291.
25 J. T. Walker, R. Haliyur, H. A. Nelson, M. Ishahak, G. Poffenberger and R. Aramandla, *et al.*, Integrated human pseudoislet system and microfluidic platform demonstrate differences in GPCR signaling in islet cells, *JCI Insight*, 2020, **5**(10), e137017.
26 J. E. Campbell and C. B. Newgard, Mechanisms controlling pancreatic islet cell function in insulin secretion, *Nat. Rev. Mol. Cell Biol.*, 2021, **22**(2), 142–158.
27 J. R. Choi, J. H. Lee, A. Xu, K. Matthews, S. Xie and S. P. Duffy, *et al.*, Monolithic hydrogel nanowells-in-microwells enabling simultaneous single cell secretion and phenotype analysis, *Lab Chip*, 2020, **20**(24), 4539–4551.
28 Y. Lu, Q. Xue, M. R. Eisele, E. S. Sulistijo, K. Brower and L. Han, *et al.*, Highly multiplexed profiling of single-cell effector functions reveals deep functional heterogeneity in response to pathogenic ligands, *Proc. Natl. Acad. Sci. U. S. A.*, 2015, **112**(7), E607–E615.
29 M. C. Liao, C. R. Muratore, T. M. Gierahn, S. E. Sullivan, P. Srikanth and P. L. De Jager, *et al.*, Single-Cell Detection of Secreted Aβ and sAPPα from Human IPSC-Derived Neurons and Astrocytes, *J. Neurosci.*, 2016, **36**(5), 1730–1746.
30 J. George and J. Wang, Assay of Genome-Wide Transcriptome and Secreted Proteins on the Same Single Immune Cells by Microfluidics and RNA Sequencing, *Anal. Chem.*, 2016, **88**(20), 10309–10315.
31 M. J. Westacott, N. W. F. Ludin and R. K. P. Benninger, Spatially Organized β-Cell Subpopulations Control Electrical Dynamics across Islets of Langerhans, *Biophys. J.*, 2017, **113**(5), 1093–1108.
32 L. S. Satin, Q. Zhang and P. Rorsman, "Take Me To Your Leader": An Electrophysiological Appraisal of the Role of Hub Cells in Pancreatic Islets, *Diabetes*, 2020, **69**(5), 830–836.
33 J. Lyon, A. F. Spigelman, P. E. Macdonald and J. E. Manning Fox, ADI IsletCore Protocols for the Isolation, Assessment and Cryopreservation of Human Pancreatic Islets of Langerhans for Research Purposes v1 [Internet], 2019, [cited 2024 Apr 4]. Available from: **https://www.protocols.io/view/adi-isletcore-protocols-for-the-isolation-assessme-x3mfqk6**.
34 N. A. J. Krentz, C. Nian and F. C. Lynn, TALEN/CRISPR-mediated eGFP knock-in add-on at the OCT4 locus does not impact differentiation of human embryonic stem cells towards endoderm, *PLoS One*, 2014, **9**(12), e114275.
35 G. Novakovsky, S. Sasaki, O. Fornes, M. E. Omur, H. Huang and C. L. Bayly, *et al.*, In silico discovery of small molecules for efficient stem cell differentiation into definitive endoderm, *Stem Cell Rep.*, 2023, **18**(3), 765–781.
36 S. Mar, E. Filatov, C. Nian, S. Sasaki, D. Zhang and F. C. Lynn, Tracking insulin- and glucagon-expressing bihormonal cells during differentiation using an INSULIN and GLUCAGON double reporter human embryonic stem cell line, *bioRxiv*, 2023, preprint, DOI: **10.1101/2023.04.19.537542**, Available from: **https://www.biorxiv.org/content/10.1101/2023.04.19.537542v1**.